Adv. Radio Sci., 5, 439–445, 2007
www.adv-radio-sci.net/5/439/2007/

Advances in Radio Science

Methods for the calibrated measurement of the scattering parameters of planar multi-port devices

I. Rolfes[1] **and B. Schiek**[2]

[1]Institut für Hochfrequenztechnik und Funksysteme, Universität Hannover, Appelstraße 9A, 30167 Hannover, Germany
[2]Institut für Hochfrequenztechnik, Ruhr-Universität Bochum, Universitätsstraße 150, 44801 Bochum, Germany

Abstract. In this article, the error-corrected determination of complex scattering parameters of multi-port devices by means of a 2-port vector network analyzer is presented. As only two ports of the device under test can be connected to the analyzer ports at a time, the remaining device ports have to be terminated by external reflections. In order to measure the scattering parameters of the DUT without the influence of systematic errors and of the external terminations, an error correction has to be performed besides the calibration. For this purpose, the application of the multi-port procedure is presented. This method has the advantage, that the external reflective terminations can be chosen arbitrarily. Furthermore, these terminations can be unknown except for one. An automatized measurement system based on a switching network is shown, which is optimized for the measurement of planar microwave circuits. An error model for the description of the measurement setup as well as a calibration procedure for the elimination of the systematic errors are presented.

1 Introduction

As vector network analyzers (VNA) with two measurement ports and four measurement channels are still widely used in laboratories and industry, methods for the error-corrected scattering parameter measurement of N-port devices ($N>2$) on the basis of a 2-port-VNA are described in this article. N-port devices, like couplers or power dividers with three or more ports can be measured with the help of a two-port network analyzer by connecting two ports of the DUT to the ports of the analyzer while the remaining $N-2$ ports of the DUT are connected to external terminations. In order to determine the complete set of scattering parameters of a multi-port as shown in Fig. 1, which is given by

$$\begin{bmatrix} b_1 \\ b_2 \\ \vdots \\ b_N \end{bmatrix} = \begin{bmatrix} S_{11} & S_{12} & \dots & S_{1N} \\ S_{21} & S_{22} & \dots & S_{2N} \\ \vdots & \vdots & \vdots & \vdots \\ S_{N1} & S_{N2} & \dots & S_{NN} \end{bmatrix} \begin{bmatrix} a_1 \\ a_2 \\ \vdots \\ a_N \end{bmatrix}, \tag{1}$$

all possible two-port combinations of the multi-port have to be measured, so that $N\cdot(N-1)/2$ two-port measurements have to be performed.

The measured scattering parameters are erroneous due to the imperfectly matched terminations having the reflection coefficients $\Gamma_3, \dots, \Gamma_N$. An error correction becomes necessary in order to eliminate the influence of the external reflections. This error correction is commonly performed according to Tippet and Speciale (1982).

In this contribution, the application of the multi-port method (Rolfes and Schiek, 2005) will be presented, which has the advantages that the external terminations can be chosen arbitrarily, e.g. short and open circuits are also applicable. Moreover, their reflection coefficients can be unknown, so that a possible inconsistency problem due to an unprecise knowledge of the terminations can be minimized. This is also known from the calibration of VNAs on the basis of self-calibration procedures (Eul and Schiek, 1991).

The contacting of multi-port devices can be performed with the help of switches (Williams and Walker, 1998). An automatized measurement setup on the basis of a switching network optimized for the characterization of planar microstrip devices with four ports is presented. For the elimination of systematic errors, the application of an adapted error model and a specific calibration procedure is described.

Correspondence to: I. Rolfes
(ilona.rolfes@rub.de)

Published by Copernicus Publications on behalf of the URSI Landesausschuss in der Bundesrepublik Deutschland e.V.

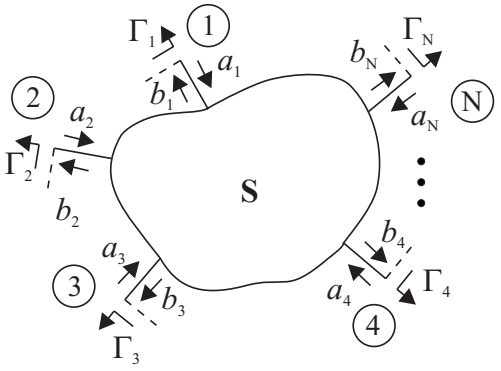

Fig. 1. Scattering and wave parameters of a N-port.

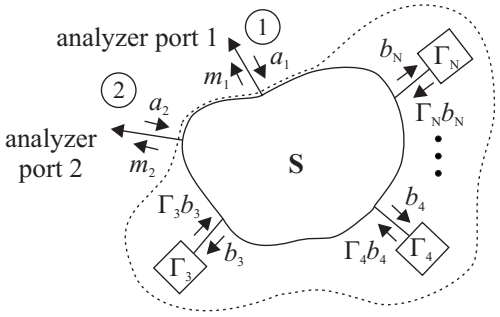

Fig. 2. Measurement of a multi-port with a 2-port VNA.

2 The multi-port method

For the characterization of N-port devices with the help of a two-port VNA only two ports of the DUT can be connected to the ports of the analyzer while the remaining ports are connected to external terminations.

In Fig. 2 a setup is shown where the connectors 1 and 2 of the DUT are connected to the VNA while the other connectors are terminated with the reflections $\Gamma_3, \ldots, \Gamma_N$. The measured and thus known wave parameters are denoted by m_i and a_i, the unknown wave parameters by b_i. Performing the measurement of all possible two-port combinations of the DUT, the complete set of measurements can be described as follows:

$$\begin{bmatrix} m_1^{(1)} & m_1^{(2)} & \ldots & b_1^{(h)} \\ m_2^{(1)} & b_2^{(2)} & \ldots & b_2^{(h)} \\ b_3^{(1)} & m_3^{(2)} & \ldots & b_3^{(h)} \\ \vdots & \vdots & \vdots & \vdots \\ b_N^{(1)} & b_N^{(2)} & \ldots & m_N^{(h)} \end{bmatrix} = \mathbf{S} \begin{bmatrix} a_1^{(1)} & a_1^{(2)} & \ldots & \Gamma_1 b_1^{(h)} \\ a_2^{(1)} & \Gamma_2 b_2^{(2)} & \ldots & \Gamma_2 b_2^{(h)} \\ \Gamma_3 b_3^{(1)} & a_3^{(2)} & \ldots & \Gamma_3 b_3^{(h)} \\ \vdots & \vdots & \vdots & \vdots \\ \Gamma_N b_N^{(1)} & \Gamma_N b_N^{(2)} & \ldots & a_N^{(h)} \end{bmatrix} \tag{2}$$

where $h{=}N{\cdot}(N{-}1)/2$. The aim of the error correction is the determination of the scattering matrix **S** of the DUT. For a brief description of the multi-port method a DUT with 3 connectors is considered here. Equation (2) can be rewritten as:

$$\begin{aligned} &\underbrace{\begin{bmatrix} b_1^{(1)} & 0 & 0 \\ 0 & b_2^{(2)} & 0 \\ 0 & 0 & b_3^{(3)} \end{bmatrix}}_{\mathbf{b}} + \underbrace{\begin{bmatrix} 0 & m_1^{(2)} & m_1^{(3)} \\ m_2^{(1)} & 0 & m_2^{(3)} \\ m_3^{(1)} & m_3^{(2)} & 0 \end{bmatrix}}_{\mathbf{M_1}} \\ &= \mathbf{S} \underbrace{\begin{bmatrix} \Gamma_1 b_1^{(1)} & 0 & 0 \\ 0 & \Gamma_2 b_2^{(2)} & 0 \\ 0 & 0 & \Gamma_3 b_3^{(3)} \end{bmatrix}}_{\Gamma\mathbf{b}} + \mathbf{S} \underbrace{\begin{bmatrix} 0 & a_1^{(2)} & a_1^{(3)} \\ a_2^{(1)} & 0 & a_2^{(3)} \\ a_3^{(1)} & a_3^{(2)} & 0 \end{bmatrix}}_{\mathbf{M_2}} \end{aligned} \tag{3}$$

resulting in a separation into known $\mathbf{M_1}, \mathbf{M_2}$, Γ and unknown parameters **S**, **b**, respectively. Introducing excitations $\tilde{a}_1^{(2)}, \tilde{a}_1^{(3)}, \tilde{a}_2^{(1)}, \tilde{a}_2^{(3)}, \tilde{a}_3^{(1)}, \tilde{a}_3^{(2)}$ with $\tilde{\mathbf{b}}{+}\tilde{\mathbf{M}}_\mathbf{1}{=}\mathbf{S}(\Gamma\tilde{\mathbf{b}}{+}\tilde{\mathbf{M}}_\mathbf{2})$ the following solution for e.g. $b_1^{(1)}$ results after some conversions:

$$\begin{aligned} b_1^{(1)} = (&\Gamma_3^{(1)}(\Gamma_2^{(3)}(a_1^{(2)}\tilde{m}_1^{(3)} - \tilde{a}_1^{(3)}m_1^{(2)}) \\ &+\tilde{\Gamma}_2^{(3)}(a_1^{(3)}m_1^{(2)} - a_1^{(2)}m_1^{(3)})) \\ &+\Gamma_2^{(1)}\Gamma_3^{(2)}(a_1^{(3)}\tilde{m}_1^{(3)} - \tilde{a}_1^{(3)}m_1^{(3)}))/D \end{aligned} \tag{4}$$

with

$$\Gamma_i^{(1)} = a_i^{(1)} - \Gamma_i m_i^{(1)}, \tag{5}$$

$$\tilde{\Gamma}_i^{(1)} = \tilde{a}_i^{(1)} - \Gamma_i \tilde{m}_i^{(1)}, \quad i = 2, 3, \tag{6}$$

and the denominator

$$D = \left(\Gamma_3^{(2)}\left(\Gamma_1^{(3)}\tilde{\Gamma}_2^{(3)} - \tilde{\Gamma}_1^{(3)}\Gamma_2^{(3)}\right)\right). \tag{7}$$

With the knowledge of **b** and under the assumption that Γ is known, matrix **S** can be determined using Eq. (3). In contrast to the method of Tippet and Speciale (1982), terminations $\Gamma_1, \ldots, \Gamma_N$ can be chosen arbitrarily for the multi-port method. Furthermore, the terminations can be unknown except for one (e.g. Γ_1), because they are calculable by:

$$\Gamma_2 = \frac{h_{11} + \Gamma_1 h_{12}}{h_{13} + \Gamma_1 h_{14}}, \qquad \Gamma_3 = \frac{h_{21} + \Gamma_1 h_{22}}{h_{23} + \Gamma_1 h_{24}}, \tag{8}$$

where the parameters h_{ij}, i=1, 2, j=1, ..., 4 are known from measurements.

By dividing the multi-port into $N{\cdot}(N{-}1)(N{-}2)/6$ subdevices with three connectors (cf. Fig. 3), the presented results can be applied to devices with more than three ports. The multi-port procedure can thus be applied iteratively to determine the complete set of scattering parameters of the N-port.

3 Automatized measurements of multi-port devices

For the automated measurements of multi-port devices with a two-port analyzer, a switching network can be used as shown exemplarily in Fig. 4 for a four-port DUT.

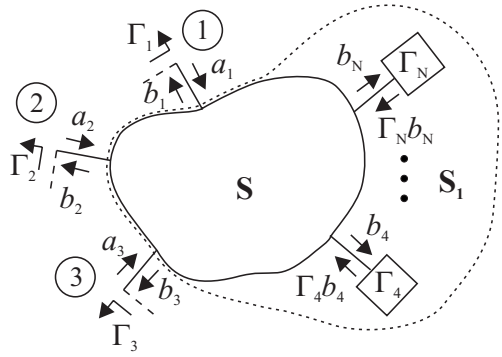

Fig. 3. Extension of the multi-port method to N-ports.

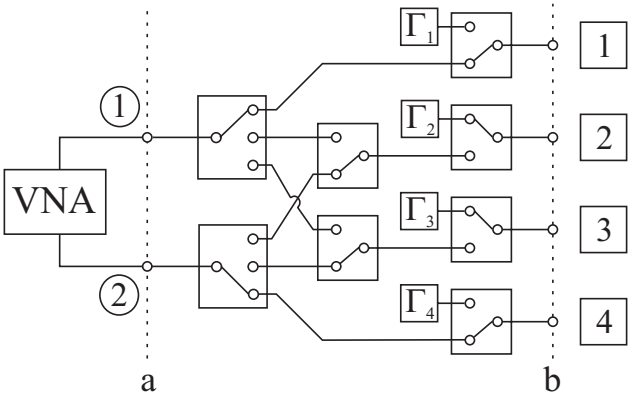

Fig. 4. Network of electro-mechanical switches for the contacting of a four-port DUT.

Using electro-mechanical switches, a two- to four-port extension of the VNA can be constructed which provides all necessary paths between the two analyzer ports and the DUT ports, needed for the complete measurement of the scattering parameters of a four-port DUT. The ports of the DUT which are not connected to the analyzer are terminated by the reflections $\Gamma_1, \ldots, \Gamma_4$.

In order to eliminate systematic errors due to transmission losses or mismatched ports, the whole setup has to be calibrated. On the basis of the 7-term error-model (Schiek and Gronefeld, 1999) of a two-port VNA with the error two-ports $\mathbf{G}^{-1}$ and $\mathbf{H}$, as shown in Fig. 5, a similar representation for the extended VNA can be derived.

For the 7-term error model of the two-port VNA in Fig. 6, the following relations between the wave parameters, the error two-ports, and the scattering matrix of the DUT hold:

$$\begin{bmatrix} b_1 \\ a_1 \end{bmatrix} = \begin{bmatrix} G_{11}\ G_{12} \\ G_{21}\ G_{22} \end{bmatrix} \begin{bmatrix} m_1 \\ m_2 \end{bmatrix} \quad , \tag{9}$$

$$\begin{bmatrix} a_2 \\ b_2 \end{bmatrix} = \begin{bmatrix} H_{11}\ H_{12} \\ H_{21}\ H_{22} \end{bmatrix} \begin{bmatrix} m_3 \\ m_4 \end{bmatrix} \quad , \tag{10}$$

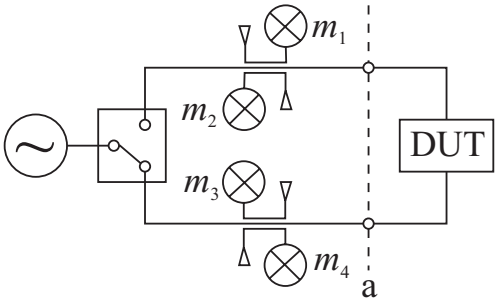

Fig. 5. Simplified setup of a two-port VNA with four measurement channels.

Fig. 6. Error model of a two-port VNA with four measurement channels on the basis of the 7-term model.

$$\begin{bmatrix} b_1 \\ b_2 \end{bmatrix} = \mathbf{S} \begin{bmatrix} a_1 \\ a_2 \end{bmatrix} \quad . \tag{11}$$

Replacing the wave parameters a_1, a_2, b_1, b_2 in Eq. (11) by the Eqs. (9), (10), the following equation results:

$$\begin{bmatrix} G_{11}m_1' + G_{12}m_2' & G_{11}m_1'' + G_{12}m_2'' \\ H_{21}m_3' + H_{22}m_4' & H_{21}m_3'' + H_{22}m_4'' \end{bmatrix} = \mathbf{S} \begin{bmatrix} G_{21}m_1' + G_{22}m_2' & G_{21}m_1'' + G_{22}m_2'' \\ H_{11}m_3' + H_{12}m_4' & H_{11}m_3'' + H_{12}m_4'' \end{bmatrix} \quad , \tag{12}$$

where $'$ and $''$ denote the two switching positions. This relation can be rearranged into a homogenous system of linear equations in dependence of the error terms:

$$\begin{bmatrix} -m_{11} & -1 & S_{11}m_{11} & S_{11} & 0 & S_{12}m_{21} & 0 & 0 \\ -m_{12} & 0 & S_{11}m_{12} & 0 & S_{12} & S_{12}m_{22} & 0 & 0 \\ 0 & 0 & S_{21}m_{11} & S_{21} & 0 & S_{22}m_{21} & 0 & -m_{21} \\ 0 & 0 & S_{21}m_{12} & 0 & S_{22} & S_{22}m_{22} & -1 & -m_{22} \end{bmatrix} \mathbf{e} = \begin{bmatrix} 0 \\ 0 \\ 0 \\ 0 \end{bmatrix} \tag{13}$$

with $\mathbf{e}=\mathbf{G_{11}}, \mathbf{G_{12}}, \mathbf{G_{21}}, \mathbf{G_{22}}, \mathbf{H_{11}}, \mathbf{H_{12}}, \mathbf{H_{21}}, \mathbf{H_{22}}]T$ and

$$[m] = \begin{bmatrix} m_{11}\, m_{12} \\ m_{21}\, m_{22} \end{bmatrix} = \begin{bmatrix} m_1' m_1'' \\ m_4' m_4'' \end{bmatrix} \begin{bmatrix} m_2' m_2'' \\ m_3' m_3'' \end{bmatrix}^{-1} \quad . \tag{14}$$

On the basis of a calibration as e.g. the TRL-method (through, reflect, line), the error terms are calculable except for a common factor. The error parameters can thus be normalized to one parameter as e.g. G_{22}, so that the following terms are known after a calibration:

$$\frac{G_{11}}{G_{22}}, \frac{G_{12}}{G_{22}}, \frac{G_{21}}{G_{22}}, \frac{H_{11}}{G_{22}}, \frac{H_{12}}{G_{22}}, \frac{H_{21}}{G_{22}}, \frac{H_{22}}{G_{22}}. \tag{15}$$

This error model can be applied to the extended VNA in Fig. 4. While the calibration of the two-port VNA is performed in the reference plane "a" in Fig. 5, the extended

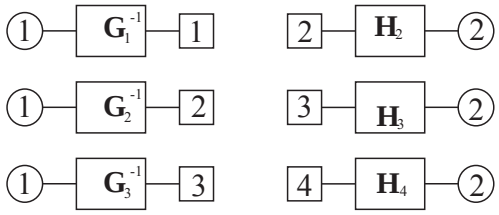

Fig. 7. Error model of the switching network.

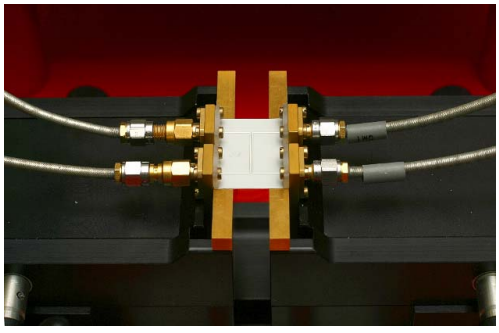

Fig. 8. Calibration structures for a microstrip four-port fixture.

VNA is calibrated in the reference plane "b" in Fig. 4. For an error description of the extended VNA, each path between the VNA ports and the ports in the plane of the DUT has to be described by an individual error two-port. For terminal 2 and 3 in plane "b", it has to be distinguished between the paths from port 1 and port 2 of the VNA resulting either in error two-ports $\mathbf{G_2}^{-1}$ and $\mathbf{H_2}$ for terminal 2 or $\mathbf{G_3}^{-1}$ and $\mathbf{H_3}$ for terminal 3. The definition of the resulting six error two-ports for the different paths is given in Fig. 7.

Assuming that a calibration is performed between port 1 and 2 in plane "b", then the error parameters of $\mathbf{G_1}$ and $\mathbf{H_2}$ are known normalized to $G_{1,22}$. The further error two-port $\mathbf{H_3}$ for example can be determined with the help of a connection between port 1 and port 3 in plane "b" in Fig. 4. The following relation results

$$\underbrace{\begin{bmatrix} m_{11} & 1 & -S_{11}m_{11} & -S_{11} \\ m_{12} & 0 & -S_{11}m_{12} & 0 \\ 0 & 0 & S_{21}m_{11} & -S_{21} \\ 0 & 0 & S_{21}m_{12} & 0 \end{bmatrix}}_{\mathbf{M_1}} \begin{bmatrix} \frac{G_{1,11}}{G_{1,22}} \\ \frac{G_{1,12}}{G_{1,22}} \\ \frac{G_{1,21}}{G_{1,22}} \\ 1 \end{bmatrix}$$

$$= \underbrace{\begin{bmatrix} 0 & S_{12}m_{21} & 0 & 0 \\ S_{12} & S_{12}m_{22} & 0 & 0 \\ 0 & S_{22}m_{21} & 0 & -m_{21} \\ S_{22} & S_{22}m_{22} & -1 & -m_{22} \end{bmatrix}}_{\mathbf{M_2}} \begin{bmatrix} \frac{H_{3,11}}{G_{1,22}} \\ \frac{H_{3,12}}{G_{1,22}} \\ \frac{H_{3,21}}{G_{1,22}} \\ \frac{H_{3,22}}{G_{1,22}} \end{bmatrix} \quad (16)$$

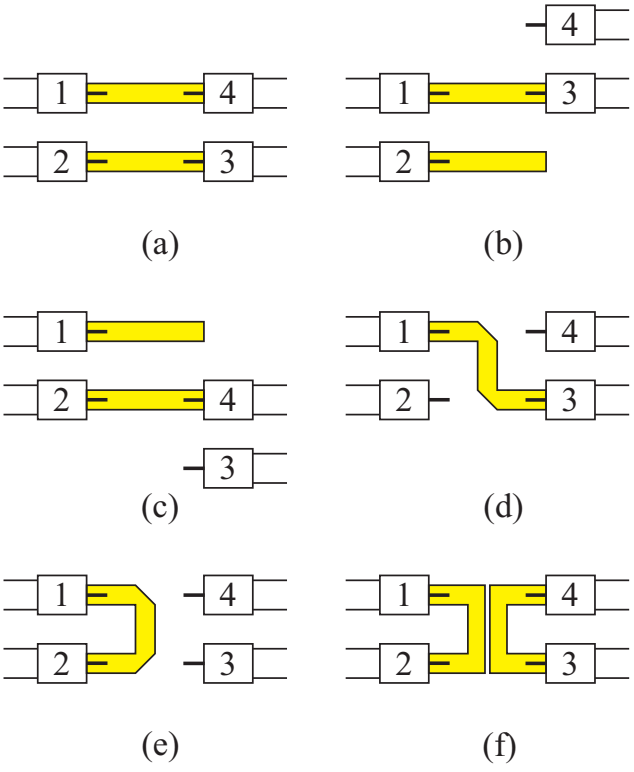

Fig. 9. Calibration structures for a microstrip four-port fixture.

which can be solved for the error parameters of $\mathbf{H_3}$, if the connection network between port 1 and 3 is either a through connection or an arbitrary but known network.

$$\begin{bmatrix} \frac{H_{3,11}}{G_{1,22}} \\ \frac{H_{3,12}}{G_{1,22}} \\ \frac{H_{3,21}}{G_{1,22}} \\ \frac{H_{3,22}}{G_{1,22}} \end{bmatrix} = \mathbf{M_2}^{-1}\mathbf{M_1} \begin{bmatrix} \frac{G_{1,11}}{G_{1,22}} \\ \frac{G_{1,12}}{G_{1,22}} \\ \frac{G_{1,21}}{G_{1,22}} \\ 1 \end{bmatrix} \quad (17)$$

In the same way the remaining error two-ports can be determined, where all error two-ports are normalized to the same parameter.

4 Measurement on microstrip substrates

In the following, the automatized measurement of planar microstrip devices will be considered. For this purpose, a commonly used test fixture for four-port devices with two of the four connectors being mounted side by side (cf. Fig. 8) is connected to the extended VNA in Fig. 4.

The scattering parameters of four-ports can thus be measured completely automatically with the help of a two-port

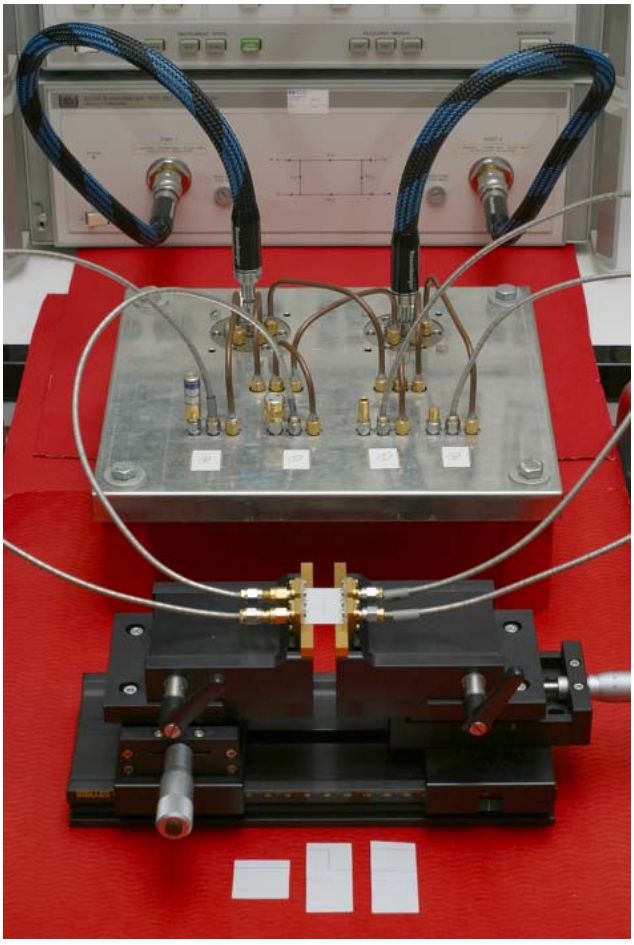

Fig. 10. Photo of the analyzer setup.

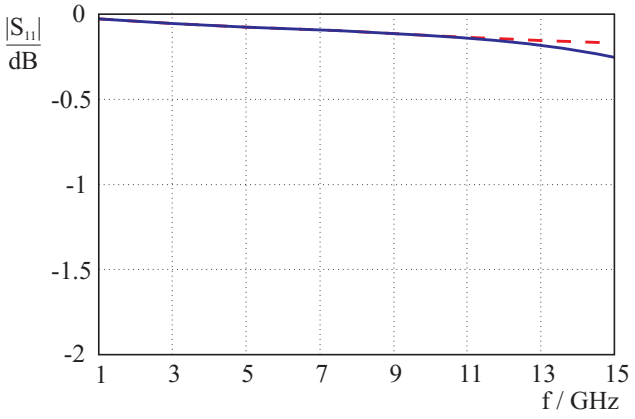

Fig. 11. Comparison of the calculated magnitude of $|S_{11}|$ of the bends with an orientation to the right (– –) and to the left (——).

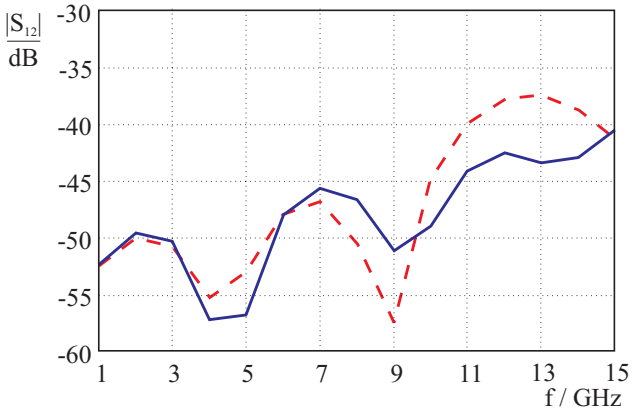

Fig. 12. Comparison of the calculated magnitude of $|S_{12}|$ of the bends with an orientation to the right (– –) and to the left (——).

VNA. A photo of the whole setup is shown in Fig. 10. The calibration of the setup is performed using microstrip calibration structures. For a setup as shown in Fig. 9, at first, a full two-port calibration can be performed between ports 1 and 4 on the basis of the TRL method. In Fig. 9a the connection of a through standard is shown exemplarily. The two error two-ports $\mathbf{G_1}$ and $\mathbf{H_4}$ of the setup can be determined. Next, contacting port 3 and port 4 to port 1 with the help of the through connection as shown in Figs. 9b and 9c, the error two-ports $\mathbf{H_3}$ and $\mathbf{G_2}$, respectively, are calculable from Eq. (17). For the determination of the remaining two-ports $\mathbf{G_3}$ and $\mathbf{H_2}$, a connection as shown in Fig. 9e is needed, in order to calculate $\mathbf{H_2}$. Due to the configuration of the connectors side by side, a connection with a through structure as before is not possible. A structure with bends becomes necessary, as shown in Fig. 9d. In order to characterize this structure, the scattering parameters are measured on the basis of the already known error two-ports $\mathbf{G_1}$ and $\mathbf{H_3}$. Assuming that this network shows the same frequency response as the structure in Fig. 9e, independently of the orientation of the bends, $\mathbf{H_2}$ is calculable. Finally, with the lower structure in Fig. 9a $\mathbf{G_3}$ can be determined, so that all error two-ports are measured with the help of the structures in Fig. 9. Thus, a calibration for the measurement of four-port microstrip devices can be performed. The calibration structures can be applied to other planar measurement setups where the contacts are positioned in a similar way as e.g. in on-wafer setups.

In order to verify the assumption that the networks in Fig. 9d and Fig. 9e show the same frequency response independently of the bend orientation a simulation by means of an electromagnetic field simulator is considered. The simulation results of the reflective and transmissive scattering parameters S_{11} and S_{12} of both networks are shown in Fig. 11 and Fig. 12. Between 1 GHz and 15 GHz, the magnitude is in close agreement, confirming the equality of the electrical characteristics of both structures.

Thus, the analyzer system is completely calibrated and a four-port DUT can be connected. The necessary measure-

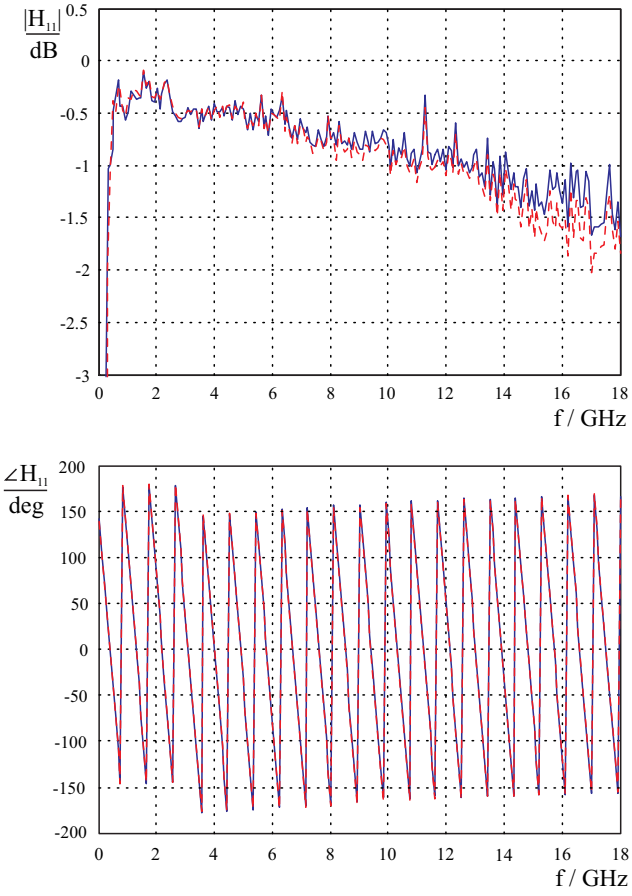

Fig. 13. Comparison of the measured error parameters of $\mathbf{H_2}$ calculated according to the presented algorithm (– –) and a full two-port calibration (——).

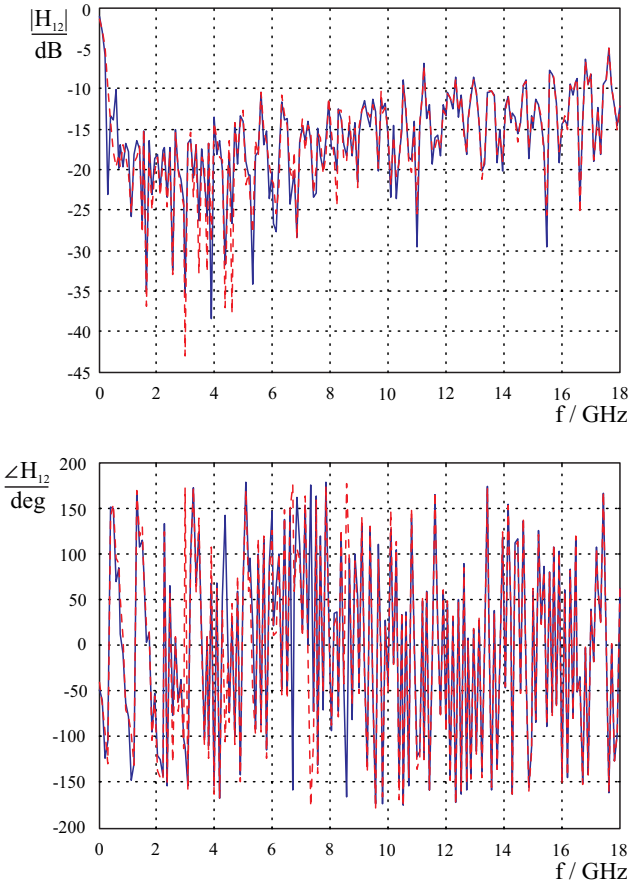

Fig. 14. Comparison of the error parameters of $\mathbf{H_2}$ calculated according to the presented algorithm (– –) and a full two-port calibration (——).

ments of the scattering parameters can then be performed fully automatized. However, a further correction procedure has to be applied in order to eliminate the errors due to the reflections of the terminations $\Gamma_1, \ldots, \Gamma_4$.

For this purpose, the multi-port method can be used advantageously. This is uncritical concerning the knowledge of the reflective characteristics of the terminations, because the frequency behavior of the terminations except for one can be determined inherently within the multi-port method. This makes this method robust. Furthermore, the multi-port method offers a high degree of freedom for the realization of the terminations. It is possible to realize the terminations as open circuits, leaving the remaining terminals of the DUT unconnected. Thus, a reduction of the complexity of the switching circuit of Fig. 4 is enabled, because the switches on the right side for the connection of the terminations $\Gamma_1, \ldots, \Gamma_4$ can be omitted.

Additionally, in order to avoid the demand for one known external termination, which is measurable with a calibrated VNA, it is also possible to determine the characteristics of this termination in combination with the measurements of the DUT by performing one additional reflection measurement. For this purpose, one further 1-port measurement has to be performed in addition to the previously mentioned two-port measurements of the DUT.

5 Measurement Results

For the verification of the previously described theory, the measurement of multi-port devices with the help of a two-port VNA, a switching network as shown in Fig. 4 on the basis of electromechanical switches is realized. Thus, the contacting procedure for the measurement of 4-port devices is completely automatized. For the calibration of the setup, a full two-port TRL-calibration is performed between ports 1 and 4 in the reference plane "b" of Fig. 4 with coaxial connectors, resulting in determination of $\mathbf{G_1}^{-1}$ and $\mathbf{H_4}$. Next, the remaining error two-ports are calculated according to the previously described theory. As an example, in Fig. 13 and Fig. 14 the calculated parameters H_{11} and H_{12} of the error

two-port $\mathbf{H_2}$, represented in a transmission matrix description, are shown in comparison to the direct determination of the error parameters of $\mathbf{H_2}$ on the basis of a full two-port TRL-calibration. Both results show good agreement over a wide frequency range.

6 Conclusions

An automatized setup for the scattering parameter measurement of multi-port devices with the help of a two-port vector network analyzer is presented. An error model for the description of the systematic errors as well as a calibration procedure optimized for the application in a microstrip test fixture are shown. The functionality of the described calibration procedure is verified by measurements. The application of the multi-port method for the correction of two-port measurements is considered.

References

Eul, H.-J. and Schiek, B.: A Generalized Theory and New Calibration Procedures for Network Analyzer Self-Calibration, IEEE Trans. Microw. Theory Tech., MTT-39, 724–731, 1991.

Ferrero, A., Sanpietro, F., and Pisani, U.: Multiport Vector Network Analyzer Calibration: A General Formulation, IEEE Trans. Microw. Theory Tech., MTT-42, 2455–2461, 1994.

Rolfes, I. and Schiek, B.: Multiport Method for the Measurement of the Scattering Parameters of N-Ports, IEEE Trans. Miccow. Theory Tech., MTT-53, 1990–1996, 2005.

Schiek, B. and Gronefeld, A.: Standing Wave Meters and Network Analyzers", Wiley Encyclopedia of Electrical and Electronics Engineering, 20, 403–423, John Wiley & Sons, 1999.

Tippet, J. C. and Speciale, R. A.: A Rigorous Technique for Measuring the Scattering Matrix of a Multiport Device with a 2-Port Network Analyzer, IEEE Trans. Microw. Theory Tech., MTT-30, 661–666, 1982.

Williams, D. F. and Walker, D. K.: In-line multiport calibrations, 51st ARFTG Dig., 88–90, 1998.